Supplementary Information (SI) for Materials Advances.

Supporting Information:

Vitamin C: Friend or Foe!

A Synopsis of Ascorbic Acid's Reduction and Oxidation of Graphene Oxide†

Omar El-Basha Hassan [a], Yves Chenavier [a], Vincent Maurel [a], Julien Pérard[b], Adnane Bouzina[a], Lionel Dubois [a] and Florence Duclairoir [a]

a. Univ. Grenoble Alpes, CEA, CNRS, Grenoble INP, IRIG, SyMMES, 38000 Grenoble, France.

b. Univ. Grenoble Alpes, CEA, CNRS, Grenoble INP, IRIG, LCBM, 38000 Grenoble, France.

Contents

GO Synthesis:

Graphite nanopowder (CAS #7782-42-5 - 400 nm APS, 99.9% purity) was bought from Nanostructured & Amorphous Materials Inc. and washed with hexane and ethyl acetate prior to using to removing any possible contaminants adsorbed on the surface of the graphite sheets. Concentrated sulfuric acid (CAS #7664-93-9 - 95-97%) and Hydrochloric acid (CAS #7647-01-0 - 37% solution) were bought from Sigma Aldrich, Sodium Nitrate (CAS #7631-99-4 - 99.7%) and Hydrogen Peroxide (CAS #7722-84-1 - 30% solution) were bought from VWR Chemical and potassium permanganate (CAS #7722-64-7 - 99%) was bought from OSI France and used as received without further purification.

3.0 g of graphite was added to a 1L beaker in an ice bath, followed by 90 ml of concentrated sulfuric acid. The mixture was kept under stirring till the temperature dropped around 4°C. At such temperature, 1.5 g of sodium nitrate was added and the mixture was left to stir for 2 h, while ensuring the temperature did not exceed 5°C. Then, 9.1 g of potassium permanganate was very slowly and carefully added not to increase the temperature above 4-5°C, and the mixture was left to stir for 90 min while maintaining the temperature between 0 and 3°C. The beaker was then removed from the ice bath and left to reach room temperature. Afterwards, 100 ml of milliQ water (18MΩ) was added slowly using a Pasteur pipette controlling that the temperature would not exceed 95°C. Then the temperature was set to 95°C and the mixture was left to stir for 2 h. The color changed from purple to brown during the course of the addition of the 100 ml of milliQ water. Another 300 ml of milliQ water was added to the mixture and the mixture was left to stir for 90 more minutes at 95°C. The heating was stopped and the mixture was allowed to cool down to room temperature. Then, 30 ml of 30% hydrogen peroxide solution was added and the mixture was left to stir for 30 min before adding 450 ml of milliQ water and leaving the mixture overnight under stirring.

Then, the brown mixture was filtered under vacuum on cellulose filter paper using fritted funnels. The precipitate was collected and re-dispersed in a 1L beaker using 900 ml of milliQ water. This suspension was then sonicated for 1 h in a water sonication bath. Afterwards, 100 ml of 37% hydrochloric acid was added and the mixture was left to stir overnight.

The upcoming steps are summarized in Figure (V.1) and detailed below. These steps were carried out to remove any acid molecules remaining, except for the last step which was meant for size selection. The size selection is carried out to remove the un-oxidized graphite as well as the less oxidized large graphene oxide sheets.

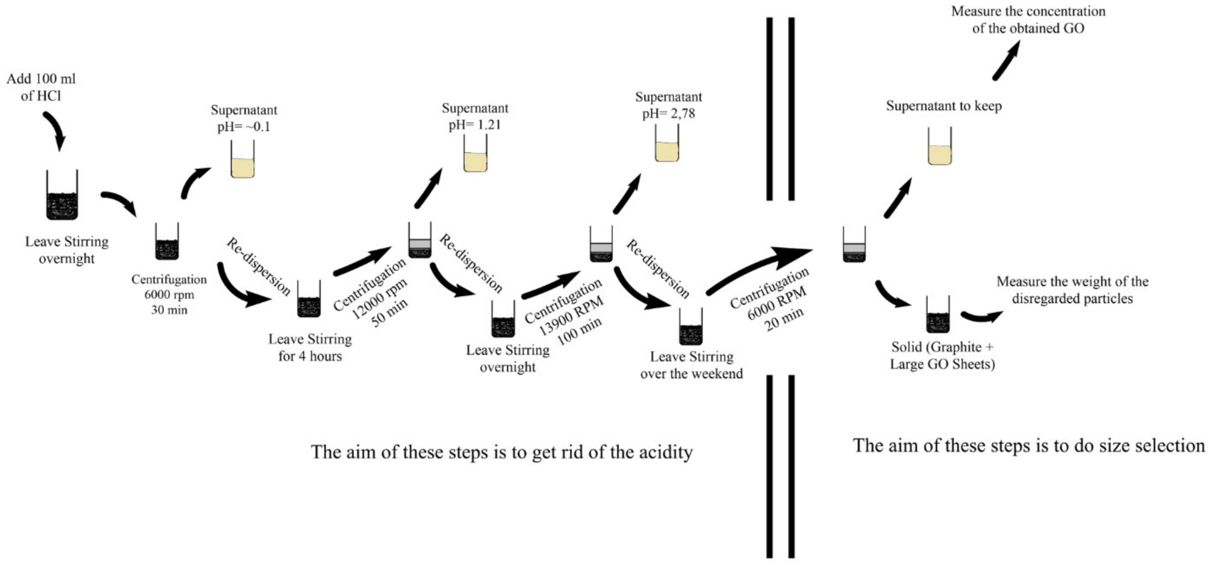

Steps for acidity removal and size selection

Synthesis of rGO-VitC samples:

L-Ascorbic Acid (L-AA) (CAS #50-81-7 - 99%) was bought from Sigma Aldrich and Ammonia solution (CAS #1336-21-6 - 28% solution) was bought from BASF and both were used as received with no further purifications prior to use.

40 ml of 5 mg/ml GO in water dispersion was placed in a round bottom flask followed by 200 ml of milliQ water (concentration of GO: 0.83 mg/ml). Two drops of 28wt.% ammonia solution was added to bring the pH between 9 and 10 (measured pH: 9.7) to promote the colloidal stability of the GO dispersion. Then, 1.08, 2.72 or 10.8 g of L-ascorbic acid was added to the mixture to make 26, 60 or 260 mM L-AA solution, respectively. A pH decrease is evidenced (~ pH 3 for all samples). The mixture was left to stir at 95°C under reflux for 30 min, 2 h or 24 h depending on the sample. The mixture was then filtered under vacuum on an ash-less cellulose filter paper (ash content < 0.01 %) using a P4 fritted glass funnel. The produced powder was then washed with copious amounts of milliQ water and with ethanol. The sample was then transferred to a cellulose thimble to be inserted in a Soxhlet set-up to further remove any traces of L-ascorbic acid. The Soxhlet purification was done with milliQ water for 48 h. The samples were then dried in an oven at 80°C overnight. The samples were stored in a desiccator with silica beads.

X-Ray Photoelectron Spectroscopy (XPS):

The XPS analysis was done using a PHI Versa Probe II spectrometer with a monochromatized Al Kα X-ray source (1486.6 eV) with a beam size of 200 µm. The samples were loaded on a conductive Cu double-faced tape surrounded by Stainless Steel (SS) rings to facilitate replenishing the surface charge state. For insulating samples like GO, double charge compensation, involving the use of an electronic charge neutralizer and an electron gun, was applied. The samples were analyzed on areas of average 200 µm2 under ultra-high vacuum. The survey spectra were acquired with a pass energy of 117.4 eV with a range from 0 to 1100 eV. The High Resolution (HR) spectra were acquired with a pass energy of 23.5 eV with ranges from 276 to 298 eV, 523 to 545 eV and 389 to 411 eV for C1s, O1s and N1s, respectively. X-ray induced secondary electron images (SXI) were recorded for each sample. The C1s sp^2/sp^3 peak at 284.3 eV was used as binding energy reference. All C/O ratios have been determined using the HR spectra atomic concentration determination. The peak fitting was done using Multipak software. Origin software was used for plotting the survey and HR spectra along with their fitted peaks.

Elemental Analysis (EA):

EA experiments were performed on a UNICUBE® organic elemental analyzer (C, H, N and S) by Elementar. The samples were loaded in Sn boats and their masses were kept between 1.5 and 2 mg. Three sample-loaded Sn boats were prepared for each sample for statistical analysis. The samples were then introduced in the oven under He gas, then burnt at 1150°C in the presence of O2, and the resulting gases were treated in a reduction tube at 850°C. The resulting gases then passed through an adsorption column where thermal programmed desorption took place at the following temperatures: 40°C for N_2, 60°C for CO_2, 150°C for H_2O and 210°C for SO_2. A thermoconductivity detector quantified the amounts of each element from the difference between the thermal conductivity of pure He gas and a mixture of He gas and the gas carrying the element of interest (ex. CO_2 for detection of C). Oxygen amount was then assumed to occupy the remaining weight percentage, after confirming the existence of only C, N and O from XPS. Origin software was used for plotting histograms of the C, H, N and O content of each sample.

Thermogravimetric Analysis (TGA):

TGA experiments were carried out using a Setaram TGA 92 equipment. The experiments were done under Ar gas from 30°C to 800°C with a heating ramp of 5 °C/min. Stabilization was done at 30°C for 30 minutes prior to heating to reach a stable mass before carrying out the analysis. Origin software was used for plotting the degradation profiles.

X-ray Diffraction (XRD):

XRD experiments were performed on a Panalytical X'pert PRO X-ray diffractometer using a Co Kα radiation source (λ=1.798 Å). The measurements were done in a θ-θ goniometer configuration in reflection mode. The samples analyzed were in the form of pellets of a diameter of 6 mm, weighing around 10-12 mg. The pellets were done through pressing the samples in a mold under 2 Tons of pressure for 15 min. The alignment prior to measurements were done using a 1/32 fixed slit, a 4 mm fixed mask, a 5 mm fixed mask and a programmable beam attenuator Fe 0.1 m with an attenuation factor of 84.96 on the incident beam side and a 0.27 receiving slit on the detector side. A ponctuel 0-D detector was used. Alignments are done for 2θ (angle between incident and reflected beams), Ω (angle between incident beam and sample's surface) and z (the height of the sample holder stage). During measurements, the 1/32 fixed slit is replaced by 1/8 fixed slit, the attenuator is stopped and the 0.27 slit was removed. The measurement was done from 3° to 60° with a step size of 0.05°. The diffractograms of the various samples were fitted using HighScore to extract the d-spacing. Origin software was used for plotting the diffractograms.

Inductively Coupled Plasma Optical Emission (ICP –OES):

Graphene samples (GO and rGO-VitC-24h) were mineralized in presence of 65% of high purity nitric acid at 55°C overnight. Samples were diluted in 10% nitric acid to a final volume of 6 ml prior to analysis by ICP-OES (Agilent 5800 VDV used in radial reading mode). A standard range of multi-elemental mix (Sigma Aldrich Periodic table mix 1) in 10% nitric acid was prepared for quantification (from 3.9 µg/L to 1 mg/L). The calibration curves (with a correlation factor of 0.999) were performed at several specific wavelengths (nm) for each element: Fe/ 234.350, 238.204, 239.563, 259.940. Mg/ 279.553, 279.800, 280.270, 285.213. Mn/ 257.610, 259.372, 260.568, 294.921. The standard deviation is less than 5% for a detection limit below 10 µg/L.

Electron Paramagnetic Resonance (EPR):

EPR experiments were done on a Bruker EMX spectrometer equipped with Bruker ER4104OR EPR resonator. The analyzed aqueous solutions were transferred into a WG-Wilmad 812-Q flat cell. The measurements were done with a microwave frequency of 9.65 GHz, a microwave Power of 20 mW, a modulation amplitude of 1.5 G and a time constant of 10 s for a total acquisition time of 18 min per sample. EasySpin MATLAB toolbox was used for simulating and fitting the EPR signals.

Table S1 Summary of the ascorbic acid reduced graphene oxide samples mentioned in literature (to the best of our knowledge)

Reaction Conditions						Results from various Characterization Techniques										
GO Conc. (mg/ml)	L-AA Conc. (mM)	Reaction Temp. (°C)	Reaction Time	pH	Special Conditions	d-spacing from XRD (nm)		I_D/I_G ratio from Raman		C/O ratio				λ_{max} of rGO from UV-VIS (nm)	Electrical conductivity (S/m)	Ref.
						GO	rGO	GO	rGO	XPS		EA				
										GO	rGO	GO	rGO			
0.1	28.4	80	24 h	Basic with NaOH	Amino Acid Stabilizer	N/A	N/A	1.56	1.75	N/A	N/A	N/A	N/A	N/A	14.1	1
1	56	95	10 min	Basic with NH_3	N/A	0.796	0.387	1.21	2.82	2	16.7	N/A	N/A	264	N/A	2
0.1	5.7	RT	48 h	Neutral	N/A	0.794	0.37	N/A	N/A	N/A	N/A	N/A	N/A	264	800	3
0.1	5.7	65	1 h	Basic with NH_3	N/A	0.93	0.358	0.92	1.12	2	4.7	N/A	N/A	263	N/A	4
2	113.6	120	6 h	N/A	Functionalized GO & Hydrothermal Synthesis	N/A	N/A	0.98	1.23	2.3	5.6	N/A	N/A	270	360	5
1	5.7	RT	48 h	N/A	N/A	0.97	0.38	0.99	1.16	N/A	N/A	0.92	2.33	N/A	N/A	6
					Thermal Treatment		0.41		1.15				2.7			
1	5.7	RT	48 h	N/A	Thermal Treatment	0.98	0.41	0.94	1.15	N/A	N/A	0.93	2.7	N/A	N/A	7
0.1	0.3-2	95	15-240 min	Basic with NH_3	N/A	N/A	N/A	N/A	N/A	2.3	12.5	N/A	N/A	268	7700	8
1	113.6	RT	10 min, 2 and 6 days	Basic with NH_4OH	N/A	N/A	N/A	N/A	N/A	N/A	N/A	N/A	N/A	268	N/A	9
N/A	100	60	30 min	Neutral	Excess H_2O_2	N/A	N/A	N/A	N/A	N/A	N/A	N/A	N/A	260	N/A	10
37	210	60	30 min	Neutral	Sonication +Excess H_2O_2	N/A	N/A	N/A	N/A	N/A	N/A	N/A	N/A	N/A	N/A	11
N/A	56.8	80	1 h	N/A	Single layered GO on Si substrate	N/A	N/A	N/A	2.3	N/A	N/A	N/A	N/A	N/A	N/A	12

0.1	22.7	25 and 60	2 and 6 h	Basic with NaOH	Ultrasonication	N/A	N/A	N/A	N/A	N/A	N/A	N/A	N/A	268	N/A	13
0.1	5.7	95	2 h	Basic with NH_3	N/A	N/A	N/A	0.95	1.19	2.65	5.15	N/A	N/A	N/A	980	14
N/A	N/A	95	1 h	Neutral	N/A	0.925	N/A	0.95	1.33	2.4	8	N/A	N/A	N/A	N/A	15
1.33	2	90	1-2 h	Basic with NH_3	N/A	0.839	0.385	0.93	1.08	N/A	6.07	N/A	N/A	N/A	N/A	16
4.0	Diff. ratios	25-80	1-3 h	Neutral to Acidic	N/A	0.862	0.377	N/A	N/A	N/A	N/A	1.13	5.16	N/A	12.1	17
2.0	57	80	1 h	N/A	N/A	0.876	0.373	N/A	N/A	N/A	N/A	N/A	N/A	N/A	800	18
0.3	28.4	RT	48 h	N/A	TiO_2 composite	N/A	N/A	1.029	1.344	N/A	N/A	N/A	N/A	N/A	N/A	19
1	56.7	RT	12 h	Basic with NH_4OH	N/A	N/A	N/A	0.89	1.15	N/A	N/A	N/A	N/A	N/A	N/A	20
N/A	N/A	50	6 h	N/A	N/A Functionalized GO	0.83 0.68	N/A	N/A	N/A	N/A	N/A	N/A	N/A	N/A	N/A	21
0.1	N/A	RT	24 h	N/A	Functionalized GO	0.83	0.44	N/A	N/A	N/A	N/A	N/A	N/A	240	N/A	22
3.0	5678	80	1 h	Neutral	Triton-X100 stabilizer	N/A	N/A	N/A	N/A	N/A	N/A	N/A	N/A	N/A	1500	23
N/A	N/A	95	1 h	Basic with NH_4OH	Spray dried (spherical particles)	N/A	N/A	N/A	N/A	N/A	N/A	N/A	N/A	290	N/A	24
2	11.4	180	12 h	N/A	Hydrothermal Synthesis	N/A	N/A	N/A	N/A	1.9	7.5	N/A	N/A	N/A	N/A	25
0.1	17.1	RT	48 h	N/A	N/A	N/A	N/A	N/A	N/A	N/A	N/A	N/A	N/A	264	N/A	26
5	568	120	N/A	N/A	Reactive Ink Printing	N/A	N/A	0.76	1.1	N/A	N/A	N/A	N/A	N/A	N/A	27
4	45.4	80	80 min	N/A	Freeze casting followed by thermal reduction at 80°C for 8h	0.905	0.35	N/A	N/A	N/A	N/A	N/A	N/A	N/A	N/A	28
3	60	90	1 h	N/A	N/A	0.806	0.355	1.09	1.3	2.3	4.7	N/A	N/A	283	N/A	29

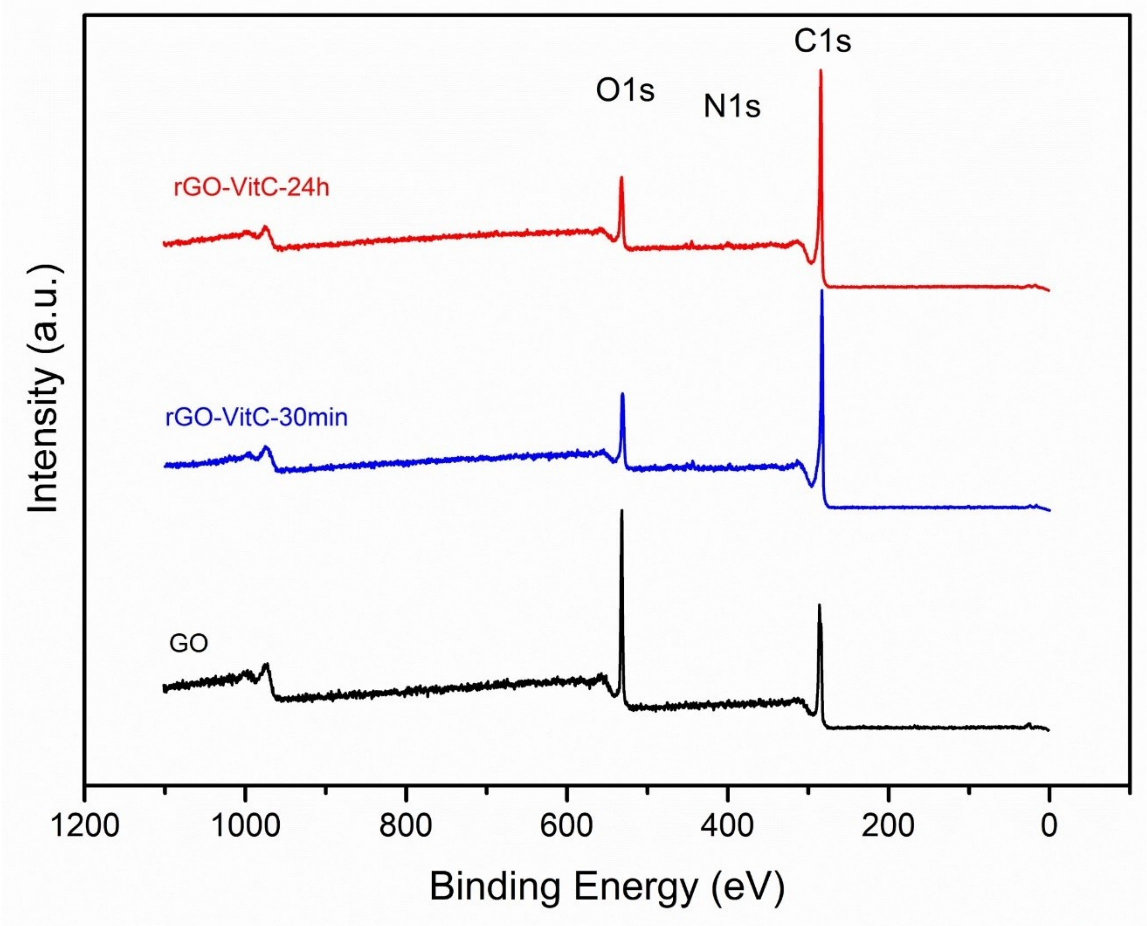

Figure S2 XPS spectra of GO, rGO-VitC-30min and rGO-VitC-24h

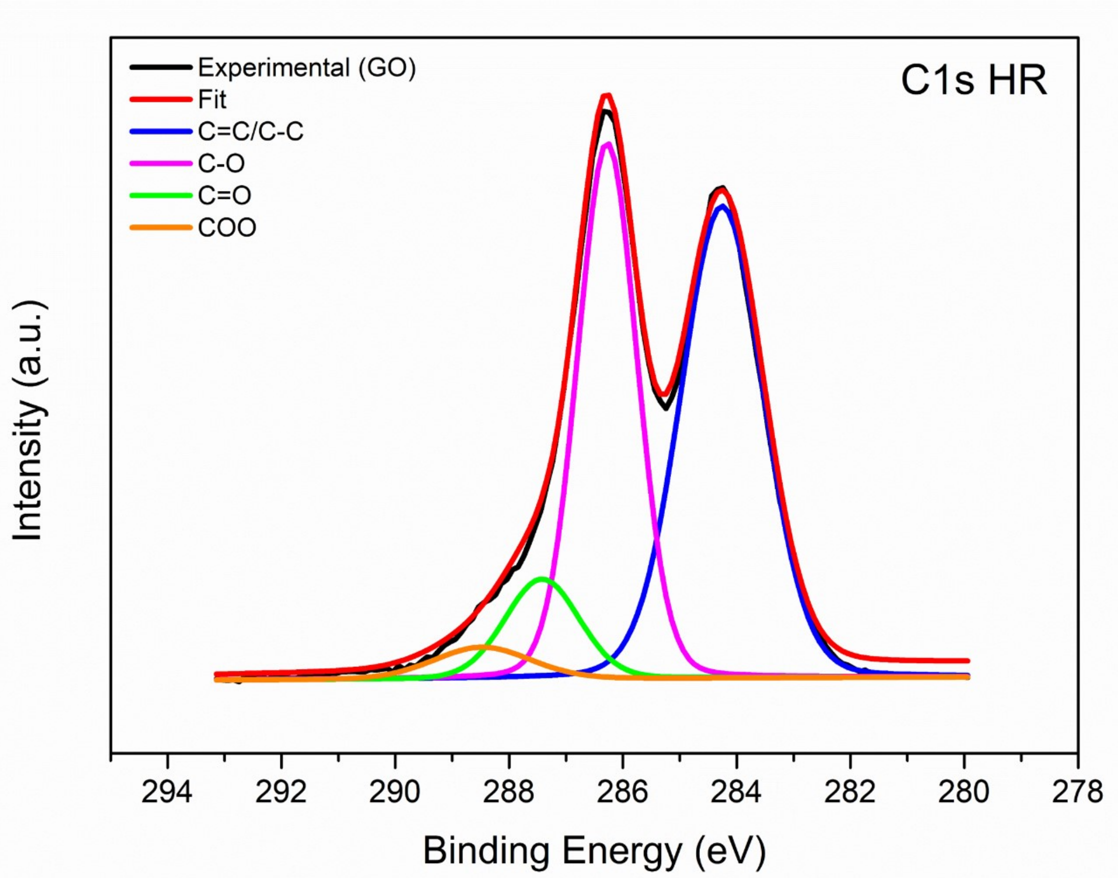

Figure S3 Fitting of the C1s HR XPS spectrum of GO

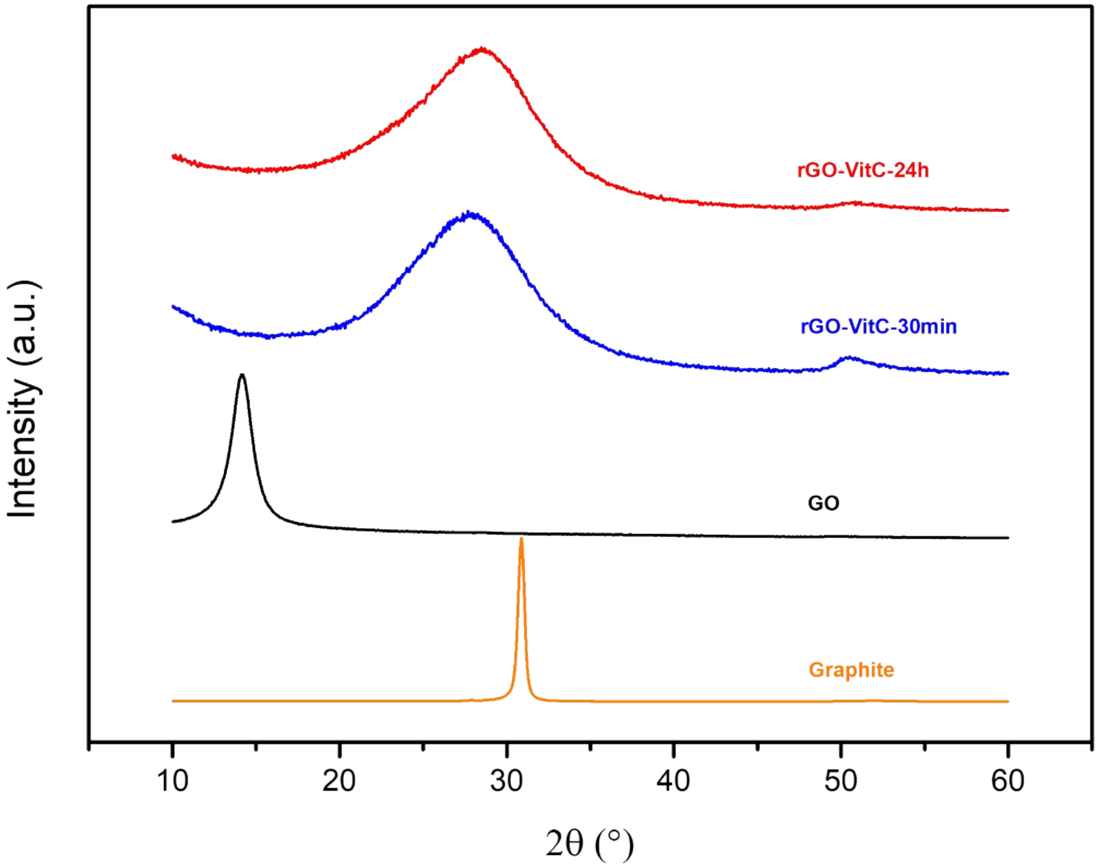

Figure S4 XRD Profiles of Graphite, GO, rGO-VitC-30min and rGO-VitC-24h

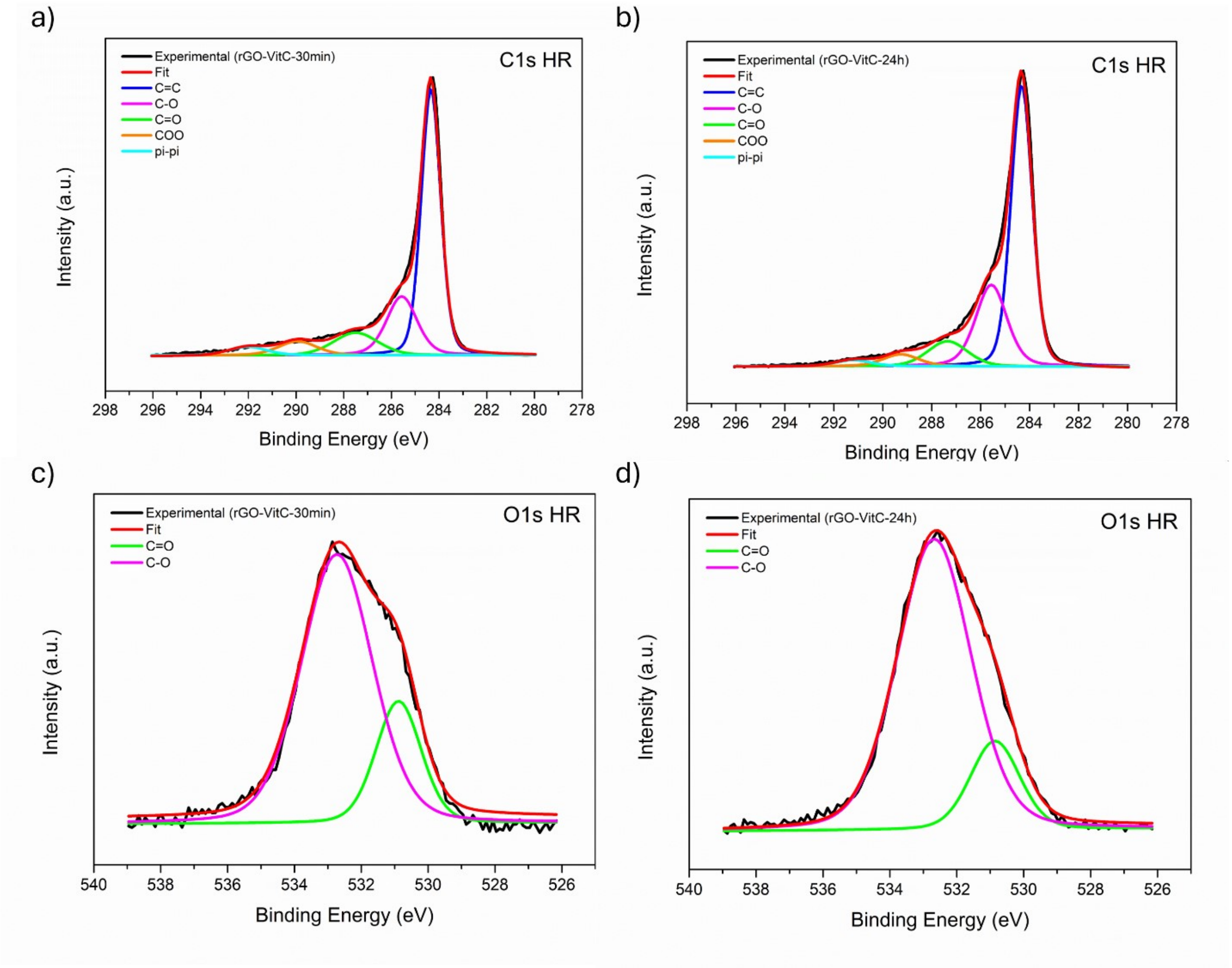

Figure S5 Fitting of C1s and O1s HR XPS peaks of (a & c) rGO-VitC-30min and (b & d) rGO-VitC-24h

Sample name	Mn (µM/mg)	Mg (µM /mg)	Zn (µM /mg)	Fe (µM /mg)
Blanc	0	0	0	0
GO	0,3 +/-0.01	0,7 +/- 0.04	1,9 +/- 0.1	0,9 +/- 0.04
RGO-VitC-24h	0,1 +/-0.005	4,6 +/- 0.1	1,3 +/- 0.06	9,9 +/- 0.1

Tables S2 Detection of metallic elements in GO and rGO-VitC-24h using ICP-OES. The calculated errors depend on the detection threshold for each element. It is 1% for values above 10µg/L and 5% for values between 1 and 10µg/L. Measurements are expressed in µM/mg of product.

This ICP-OES analysis was conducted at different dilutions, but only the results obtained for one are presented. The analysis showed the presence of Mn, Mg, Zn and Fe in GO, and rGO-VitC-24h. Ca and Si have also been found in both sample (not shown to keep the focus on metals that could be reactive towards L-AA oxidation).

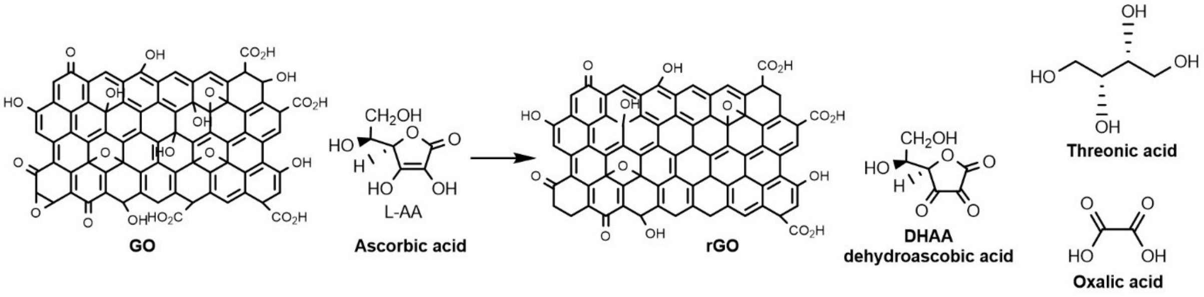

Scheme S6 Intermediates and by-products for GO reduction with L-AA

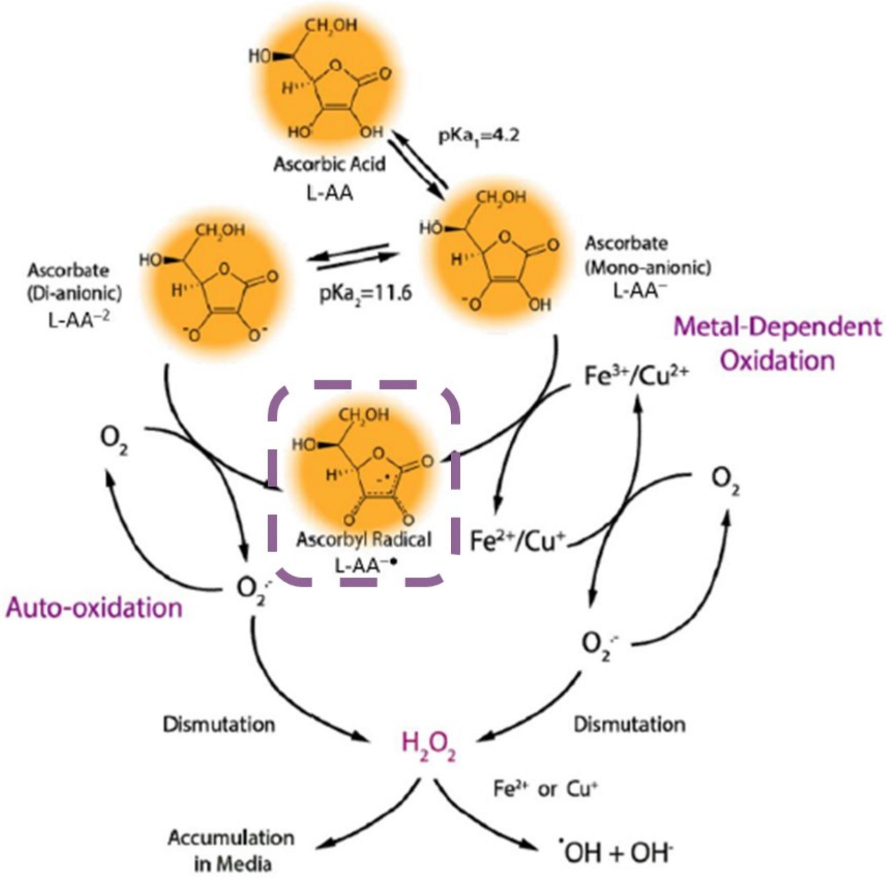

Scheme S7 Intermediates and by-products for L-AA auto- or metal-catalyzed oxidation[30]

References:

1 J. Gao, F. Liu, Y. Liu, N. Ma, Z. Wang and X. Zhang, *Chem. Mater.*, 2010, **22**, 2213–2218.

2 D. He, L. Shen, X. Zhang, Y. Wang, N. Bao and H. H. Kung, *AIChE Journal*, 2014, **60**, 2757–2764.

3 J. Zhang, H. Yang, G. Shen, P. Cheng, J. Zhang and S. Guo, *Chem. Commun.*, 2010, **46**, 1112–1114.

4 K. K. H. De Silva, H.-H. Huang and M. Yoshimura, *Appl. Surf. Sci.*, 2018, **447**, 338–346.

5 H. Su, P. Zhu, L. Zhang, F. Zhou, X. Liang, T. Li, Q. Wang, R. Sun and C. Wong, *Sustainable Energy Fuels*, 2017, **1**, 1601–1610.

6 M. P. Lavin-Lopez, A. Paton-Carrero, L. Sanchez-Silva, J. L. Valverde and A. Romero, *Adv. Powder Technol.*, 2017, **28**, 3195–3203.

7 M. P. Lavin-Lopez, J. L. Valverde, A. de Lucas-Consuegra, A. B. Calcerrada, A. Paton-Carrero and A. Romero, *Mater. Sci. Technol.*, 2019, **35**, 361–367.

8 M. J. Fernández-Merino, L. Guardia, J. I. Paredes, S. Villar-Rodil, P. Solís-Fernández, A. Martínez-Alonso and J. M. D. Tascón, *J. Phys. Chem. C*, 2010, **114**, 6426–6432.

9 M. A. Velasco-Soto, S. A. Pérez-García, J. Alvarez-Quintana, Y. Cao, L. Nyborg and L. Licea-Jiménez, *Carbon*, 2015, **93**, 967–973.

10 X. Zhu, Q. Liu, X. Zhu, C. Li, M. Xu and Y. Liang, *Int. J. Electrochem. Sci.*, 2012, **7**, 5172–5184.

11 I. O. Faniyi, O. Fasakin, B. Olofinjana, A. S. Adekunle, T. V. Oluwasusi, M. A. Eleruja and E. O. B. Ajayi, *SN Appl. Sci.*, 2019, **1**, 1181.

12 S. Eigler, S. Grimm, M. Enzelberger-Heim, P. Müller and A. Hirsch, *Chem. Commun.*, 2013, **49**, 7391–7393.

13 A. Abulizi, K. Okitsu and J.-J. Zhu, *Ultrason. Sonochem.*, 2014, **21**, 1174–1181.

14 C. Xu, X. Shi, A. Ji, L. Shi, C. Zhou and Y. Cui, *PLOS ONE*, 2015, **10**, e0144842.

15 S. Abdolhosseinzadeh, H. Asgharzadeh and H. Seop Kim, *Sci Rep*, 2015, **5**, 10160.

16 M. Fathy, A. Gomaa, F. A. Taher, M. M. El-Fass and A. E.-H. B. Kashyout, *J Mater Sci*, 2016, **51**, 5664–5675.

17 Z. Sui, X. Zhang, Y. Lei and Y. Luo, *Carbon*, 2011, **49**, 4314–4321.

18 J. Li, J. Li, L. Li, M. Yu, H. Ma and B. Zhang, *J. Mater. Chem. A*, 2014, **2**, 6359–6362.

19 H. Ding, S. Zhang, J.-T. Chen, X.-P. Hu, Z.-F. Du, Y.-X. Qiu and D.-L. Zhao, *Thin Solid Films*, 2015, **584**, 29–36.

20 Y. Liu, S. Luo, S. Yan, J. Feng and T. Yi, *Ionics*, 2020, **26**, 415–422.

21 A. Pruna, D. Pullini and D. Busquets, *Int. J. Mat. and Metall. Eng.*, 2013, **7**, 789–792.

22 A. Pruna, D. Pullini and D. Busquets, *J. Nanopart. Res.*, 2013, **15**, 1605.

23 V. Dua, S. P. Surwade, S. Ammu, S. R. Agnihotra, S. Jain, K. E. Roberts, S. Park, R. S. Ruoff and S. K. Manohar, *Angew. Chem. Int. Ed.*, 2010, **49**, 2154–2157.

24 T. Ha, S. K. Kim, J.-W. Choi, H. Chang and H. D. Jang, *Adv. Powder Technol.*, 2019, **30**, 18–22.

25 M. Serrapede, M. Fontana, A. Gigot, M. Armandi, G. Biasotto, E. Tresso and P. Rivolo, *Materials*, 2020, **13**, 594.

26 W. Chartarrayawadee, S. E. Moulton, C. O. Too, B. C. Kim, R. Yepuri, T. Romeo and G. G. Wallace, *J. Appl. Electrochem.*, 2013, **43**, 865–877.

27 Z. Stempien, M. Khalid, M. Kozicki, M. Kozanecki, H. Varela, P. Filipczak, R. Pawlak, E. .Korzeniewska and E. Sąsiadek, Synth. Met., 2019, **256**, 116144.

28 S. P. Lee, G. A. M. Ali, H. H. Hegazy, H. N. Lim and K. F. Chong, *Energy Fuels*, 2021, **35**, 4559–4569.

29 J. Indujalekshmi, P. Krishnan, R. V. Reji and V. Biju, *Mater. Today: Proc.*, DOI:10.1016/j.matpr.2023.02.159.

30 A. J. Michels and B. Frei, Nutrients, 2013, 5, 5161–5192.